Eur. Phys. J. Special Topics **164**, 127–139 (2008)

DOI: 10.1140/epjst/e2008-00839-y

THE EUROPEAN PHYSICAL JOURNAL
SPECIAL TOPICS

Identifying spatial pattern of NDVI series dynamics using recurrence quantification analysis

A case study in the region around Beijing, China

S.C. Li[1,a], Z.Q. Zhao[1,2], and F.Y. Liu[1]

[1] College of Urban and Environmental Sciences, Peking University, 100871 Beijing, China
[2] The Key Laboratory for Environmental and Urban Sciences, Shenzhen Graduate School, Peking University, 518055 Shenzhen, China

Abstract. Ecosystem is a prototypical complex system, exhibiting a non-stationary temporal dynamics and complicated spatial patterns, the characterization and description of which is riddled with challenges. In this paper recurrence quantification analysis (RQA), an extended branch of recurrence plots (RPs), was used to measure the determinism and predictability of Normalized Difference Vegetation Index (NDVI) series and its spatial patterns. After introducing the theoretical background of RPs and RQA indices, the implementation of this methodology was demonstrated using NDVI data of region around Beijing, China. The results show that the RQA indices can efficiently capture the nonlinear features of NDVI series and explicitly identify the spatial patterns. The temporal variation and dynamics of NDVI series shows significant spatial differences with the change of landuse and landcover types, characterizing by higher determinism and predictability in natural ecosystem and lower determinism and predictability in agricultural ecosystem. The research work indicates that combination of recurrence quantification analysis and geographical information system can offer an alternative approach to identifying the spatial pattern of temporal NDVI series dynamics.

1 Introduction

From an ecosystem management perspective, understanding and characterising the dynamic regime of an ecosystem is of utmost importance in order to be able to track and quantify the effects of disturbance on a given system [1]. Ecosystem is a prototypical complex system, exhibiting all of the key attributes commonly attributed to a complex system, including: dissipative structure, non-linear dynamics, self-organization, emergence, and critical phase transition. When ecosystems and their constituent populations emerge attributes of complex system, conventional methods might fail to detect relationships between ecological and environmental variables simply because their underlying assumption of linearity is violated [2], resulting in poor insights regarding underlying physical processes and evolution trends. Finding robust methods for quantifying non-linear dynamics in the presence of noise, non-stationarity, and short data series is an active area of research in many disciplines [3].

In recent years, some nonlinear approaches have been used to express the characteristics of ecosystem, such as the correlation dimension, Lyapunov exponents, Kolmogorov entropy,

[a] e-mail: scli@urban.pku.edu.cn

approximate entropy, sample entropy, etc. However, most of these methods need long data series. The uncritical application of these methods especially to natural data often leads to pitfalls [4,5]. To successfully investigate such complex ecosystem it seems best to use non-linear tools that are independent of prescribed statistical distributions of the data, can deal with short data sets, are not stymied by actual signal transients and outliers, and can project the input signal into higher dimensional space. Up to date, recurrence analysis seems to fit the bill in all of these important aspects [6]. The recurrence plots (RPs) is a methods of analysis of data that was initially introduced to visualize the behavior of a trajectory of a dynamical system in phase space [5,7]. The RPs-based techniques have been successfully applied to various fields such as biology [8], earth science [9] and so on.

The challenge of characterisation is compounded not only by the complexity of ecosystem dynamics, but also by a general lack of data that cover the range of temporal and spatial scales over which ecosystem processes operate [1]. Fortunately, broad coverage, low cost, multi-temporal and repetitive satellite data may offer a beneficial supplement for field observational data in mapping and monitoring the dynamics of ecosystem. In this study, a long-term satellite remote sensing data product, NOAA AVHRR NDVI data, were employed to investigate the determinism and predictability of landcover variation.

The objective of this paper is to characterize spatial patterns in the Beijing region through the quantification of temporal NDVI dynamics with the use of recurrence plots and recurrence quantification analysis. The paper is organized as follows. The data and geographical features of study area will be briefly described in section 2. In section 3, the theoretical background and algorithm of Recurrence Plots and applied to the data will be explained. section 4 presents results of investigation of RPs and RQA. In section 5 we summarize our results and give a briefly conclusion and discussion.

2 Study area and data

2.1 Study area

The study area is located in the north of China (Fig. 1) and covers an areal extent of approximately 182,600 km^2. It consists of three different physiographical regions, i.e. plain in south, mountain in north, and plateau in northwest. The elevation ranges from −1 m (costal zone in east) to 2500 m (mountain in north). The climate type in study area is warm and temperate zone semi-humid continental monsoon climate with clear four seasons. It is rainy and hot in summer while cold and dry in winter. Annual temperature ranges from −3 °C to 14 °C, and annual precipitation ranges from 320 to 773 mm. The precipitation of the growing season (April to September) accounts for about 90% of the total annual precipitation, and the variation between years is large. Precipitation is the limiting factor for the natural vegetation during the growing period. According to the regional vegetation map of China, the types of vegetation in study area are mainly composed by warm and temperate zone deciduous broadleaved forest dominated by the *Quercus, Tilia, Fraxinus, Aceraceae, Poplarsand* and the conifer forest dominated by the *Pinus tabulaeformis* and *Platycladus orientalis*. However, long-term extensive human activities including deforestation, farmland clearing, and urbanization have altered the original vegetation as well as its character. Land cover and landuse types in plain region are cropland, wetland and urban built-up area.

2.2 Data acquisition

One of the most widely used indices for green cover monitoring is the Normalized Difference Vegetation Index (NDVI) [10–14]. It is computed by the product of the ratio of two electromagnetic wavelengths (near infrared − red)/(near infrared + red). For the data sensed

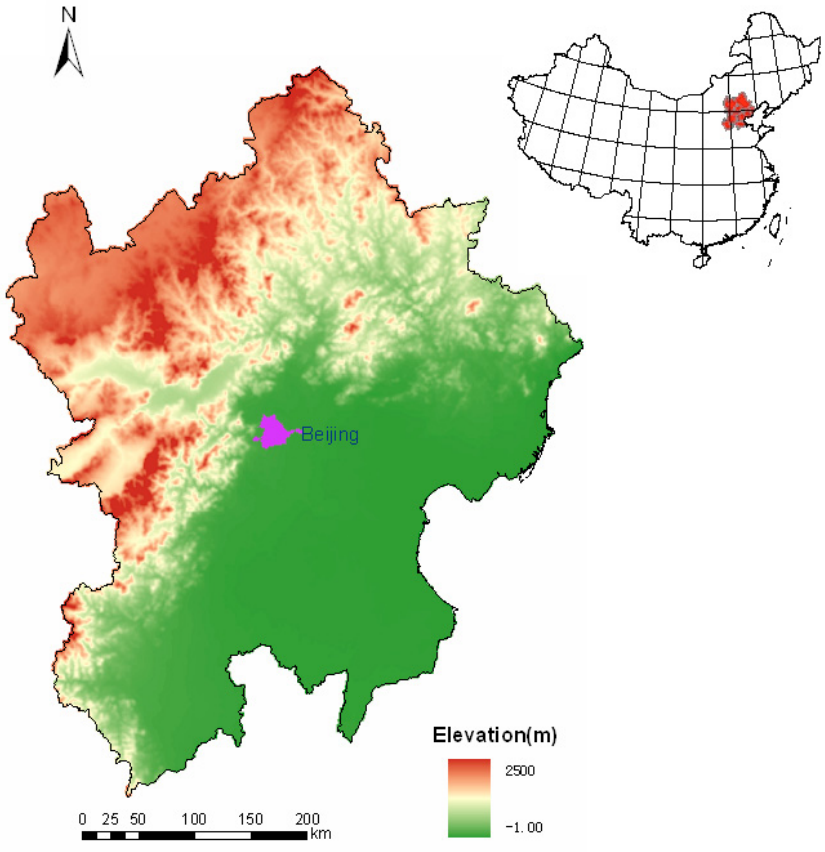

Fig. 1. The geographical location of study area.

by NOAA–AVHRR it is calculated as the normalized ratio between channel 1 and channel 2.

$$\text{NDVI} = (\text{Channel 2} - \text{Channel 1})/(\text{Channel 2} + \text{Channel 1})$$

Channel 1 is in a part of the spectrum where chlorophyll causes considerable absorption of incoming radiation, and Channel 2 is in a spectral region where spongy mesophyll leaf structure leads to considerable reflectance.

NDVI provides a measure of the amount and vigor of vegetation at the land surface. The magnitude of NDVI is related to the level of photosynthetic activity in the observed vegetation.

For this study, we used a NDVI time series of satellite observations at 8-km ($64\,\text{km}^2$) spatial and 15-day temporal resolution, covering the period from August 1981 to December 2003 produced by the Global Inventory Modeling and Mapping Studies (GIMMS) group from measurements of the advanced very high resolution radiometer (AVHRR) onboard the NOAA 7, NOAA 9, NOAA 11, and NOAA 14 satellites. NOAA AVHRR sensors have been operational for more than two decades and offer a length of record that is unmatched. This NDVI time series has been corrected for residual sensor degradation and sensor intercalibration differences, effects of changing solar zenith and viewing angles, volcanic aerosols, atmospheric water vapor and cloud cover, using nonlinear empirical mode decomposition methods [15].

NDVI has a theoretical range between -1 and $+1$, though the observed range is usually smaller. Non-vegetated materials generally have a much lower NDVI than dense vegetation, since their reflectance in the nearinfrared and visible bands are more nearly equal. Values of NDVI for vegetated land generally range from about 0.1 to 0.7, with values greater than 0.5 indicating dense vegetation.

3 Methods and analytical procedures

3.1 Methods

3.1.1 Recurrence plots and recurrence quantification analysis

Recurrence Plots (RPs) was firstly introduced by Eckman [16] to visualize the time dependent behaviour of the dynamical system. The RP is defined by

$$\mathrm{R}_{i,j}(\varepsilon) = \Theta\left(\varepsilon - \|\mathbf{x}_i - \mathbf{x}_j\|\right), \qquad i,j = 1,\ldots,N \tag{1}$$

where N is the number of measured points $\mathbf{x}_i$, ε is a small threshold distance, $\|\cdot\|$ is a norm, and $\Theta(\cdot)$ the Heaviside function. The phase space vectors for one dimensional time series u_i from observations is generally reconstructed by using Taken's time delay method $\mathbf{x}_i = (u_i, u_{i+\tau}, \ldots, u_{i+(m-1)\tau})$ with embedding dimension m and delay time τ, and the embedding dimension is usually estimated by using false neighbor method. Every point of the phase space trajectory x_i is tested whether it is close to another point of the trajectory x_j, i.e. the distance between these two points is less than a specified threshold ε. The recurrence states at time i and time j could be marked by black points if $R_{i,j} \equiv 1$ or a white points if $R_{i,j} \equiv 0$ in a two dimensional square array.

Fig. 2(a) shows the homogeneous RPs structure of white noise, characterized by mainly single points, which is typical for independent stochastic systems, as the state at time $i+1$ is unrelated to the one at time i. Figure 2(b) represents a sine function, i.e. a circle in phase space. Its RPs is then characterized by non-interrupted diagonal lines, and indicates the high determinism [17].

To overcome the limitations of qualitative description of RPs, Zbilut, Webber and some other scholars [18–20] extended the RPs to recurrence quantification analysis (RQA), and defined measures of complexity using the recurrence point density, diagonal lines, and vertical lines in the recurrence plots.

Determinism (DET) is a ratio of recurrence points that form diagonal structure to all recurrence points, and is a measure of the determinism or predictability of the system. $\%DET$ is about zero for a random series and close to 100 for a deterministic series.

$$DET = \frac{\sum_{l=l_{\min}}^{N} lP(l)}{\sum_{l=1}^{N} lP(l)}. \tag{2}$$

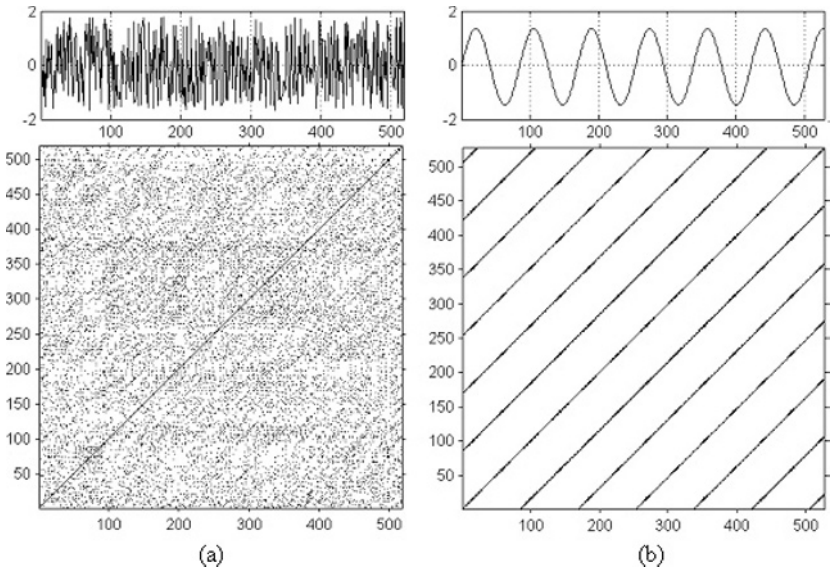

Fig. 2. Prototypical examples of RPs: (a) RP of white noise, (b) RP of a sine function.

Bloh et al. proposed Rényi entropy of second order K_2 to indicate the long-term predictability of time series [17]. Usually, K_2 is estimated by using recurrence quantification analysis according to the following relationship [21]

$$P_{\varepsilon}^{c}(l) \sim \varepsilon^{D_2} \exp\left(-\hat{K}_2(\varepsilon)\tau l\right), \tag{3}$$

where $P_{\varepsilon}^{c}(l)$ is the cumulative distribution of diagonal lines in the RPs, and $\hat{K}_2$ is an estimator of K_2. D_2 is the correlation dimension of the system under consideration. For a perfect deterministic system there is only one possibility for the trajectory to evolve, and therefore $K_2 = 0$. Conversely, for a pure stochastic systems the number of possible future trajectories increases to infinity so fast, that $K_2 \to \infty$. Chaotic systems are characterized by a finite intervenient value of K_2 between deterministic and stochastic system. The inverse of K_2 has units of time and can be interpreted as the mean prediction horizon/time of the system [17,21,22].

3.1.2 Embedding dimension, delay time, and thresholds

It is quite obvious that the topological structures of recurrence plot and indices of recurrence quantification analysis depend strongly on embedding dimension m, delay time τ, and thresholds ε. To determine τ, average mutual information of time series is computed. The method of mutual information for finding the delay τ was proposed by Fraser and Swinney [23]. It is also important to correctly estimate the embedding dimension of the time series. If the embedding is done correctly, the system dynamic is invariant and certain properties of the original system are preserved in the embedded space. The number of false nearest neighbors analysis is usually used to obtain the embedding dimension d [24]. The threshold ε is also crucial parameter in recurrence plots analysis. If ε is not being chosen properly, too small or to large, the spurious structures will appear in RPs. The some methods for the choice of the threshold ε include mean or maximum phase space diameter, recurrence point density, and standard deviation of the observational noise [7].

3.1.3 Geographical information system

A geographic information system (GIS) is any system for capturing, storing, analyzing and managing geographically referenced data and information. GIS is a visual computer platform that allows users to create interactive queries, analyze the spatial information, edit data, maps, and present the results of all these operations. In this study we used ArcGIS 9.2 (ESRI Inc., 1999–2006) software to perform spatial analysis, manage large amounts of spatial data, and produce cartographically appealing maps of recurrence quantification analysis.

3.2 Analytical procedures

3.2.1 Projection transform

The original GIMMS NDVI data is in an 8 km Albers Equal Area Conic projection using the Clarke 1866 ellipsoid with the central meridian 75°E. To match with other data layers such as landuse and vegetation, NDVI was transformed into Albers Conical Equal Area Conic projection using Krasovsky 1940 ellipsoid with the central meridian 105°E, First standard parallel 25°N and Second standard parallel 47°N in ArcGIS.

3.2.2 NDVI series extraction

Further processing step after the reprojection was to extract NDVI data of study area. The boundary coverage of Beijing and adjacent area was used to clip out the study area from

Table 1. The geographical characters of selected NDVI time series.

Land cover	Longitude	Latitude	Sampling site	Land use
Woodland	117°2′10″E	41°1′11″N	Fengning County, Hebei Province	Cropland in valley floor
Grassland	114°32′20″E	41°25′42″N	Zhangbei County, Hebei Province	Dry farming
Cropland	116°33′34″E	38°53′17″N	Wenan County, Hebei Province	Irrigated farming

the re-projectioned NDVI grid images. NDVI values for all pixels were then extracted in grid format from each AVHRR image using ArcGIS Command *Extract by Mask*. Original NDVI images were converted into DBF file format using GIS Command *Raster to Features* in Spatial Module, generating 538 × 2837 data matrix, i.e. total 2837 NDVI series with 538 data points.

To more clearly visualize RPs structures of NDVI time series in different land cover regions, three sampling sites, represented woodland, grassland, and cropland respectively, were chosen (Table 1) with 15 km circle buffer, and NDVI values were extracted.

3.2.3 RPs and RQA of NDVI series

RPs and RQA-based indices, DET and K_2, for all NDVI series were performed by using CRP toolbox for Matlab (provided by TOCSY: http://tocsy.agnld.uni-potsdam.de). The parameters of RPs and RQA measures were embedding dimension $m = 4$, time delay $\tau = 6$, which were determined by false nearest neighbor analysis and average mutual information computation respectively (Fig. 3 and Fig. 4). The method for finding the neighbors of the phase space trajectory was fixed amount of nearest neighbors, and the threshold ε was 0.05.

Above mentioned analytical processes can be illustrated by Fig. 5. Fig. 5(a) denotes that multi-temporal NDVI images of study area were clipped out. Fig. 5(b) represents the extraction of all NDVI pixel values for each NDVI images, and generating NDVI data sets with matrix size 538 × 2837. Fig. 5(c) presents the computation of DET and K_2, and interpolation for the formation spatial pattern in GIS.

4 Results

4.1 Recurrence plots of selected NDVI series

The dynamic characters of the three selected NDVI series can be differentiated by comparing their recurrence plots (Fig. 6, Fig. 7 and Fig. 8), in which recurrence patterns are visible

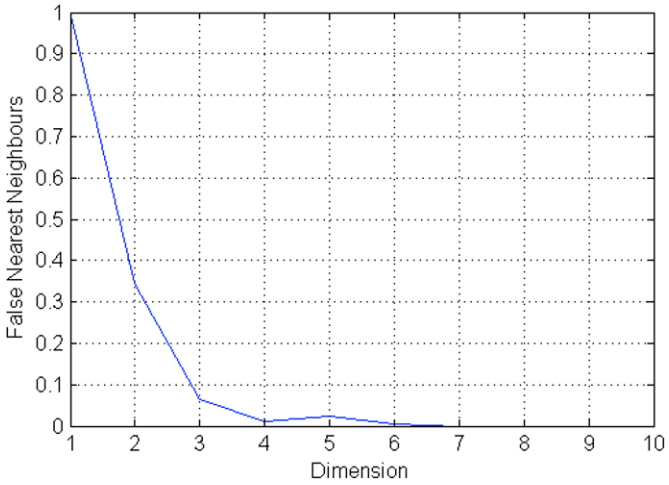

Fig. 3. Determining embedding dimension by false nearest neighbors analysis.

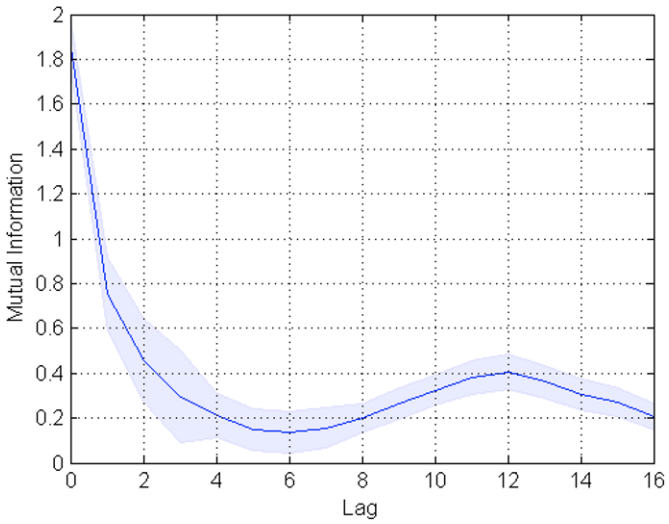

Fig. 4. Determining delay time by average mutual information computation.

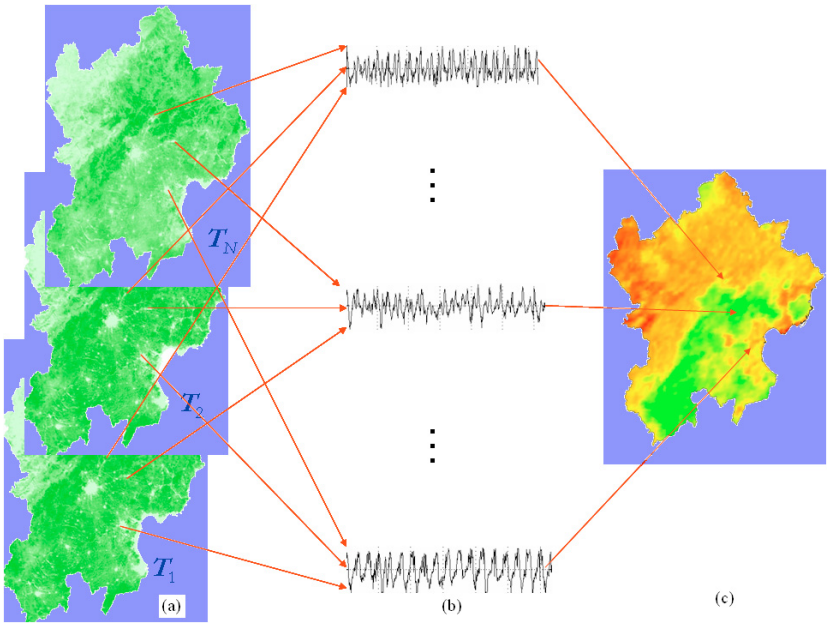

Fig. 5. The flowchart for analyzing the spatial pattern of NDVI series dynamics.

different. Long diagonal lines structuring in woodland NDVI series seems to be more common than that in the grassland and cropland NDVI series, suggesting higher predictability in woodland NDVI series than in latter NDVI series. A significant break-up of observable structure with increasing disturbance frequency can be noted in both Fig. 7 and Fig. 8, especially in RPs of cropland NDVI series in 1990, 1993 and 1997, indicating more intensive disturbance was imposed upon cropland and grassland NDVI series. Because analysis of the structures in recurrence plots is largely a qualitative visual inspection, these first impressions must be confirmed by recurrence quantification analysis. The RQA indices were calculated for the plots shown in Fig. 6, Fig. 7 and Fig. 8, and were given in Table 2. The NDVI series in cropland region is also less deterministic, (lower *DET* value), a reflection of its greater inter-annual irregularity.

Table 2. RQA indices of selected NDVI series.

Region	*DET* (%)	*L*	*LAM* (%)	*TT*
Woodland	72.35	3.02	54.47	2.18
Grassland	65.95	2.95	61.74	2.32
Cropland	57.28	2.78	58.96	2.42

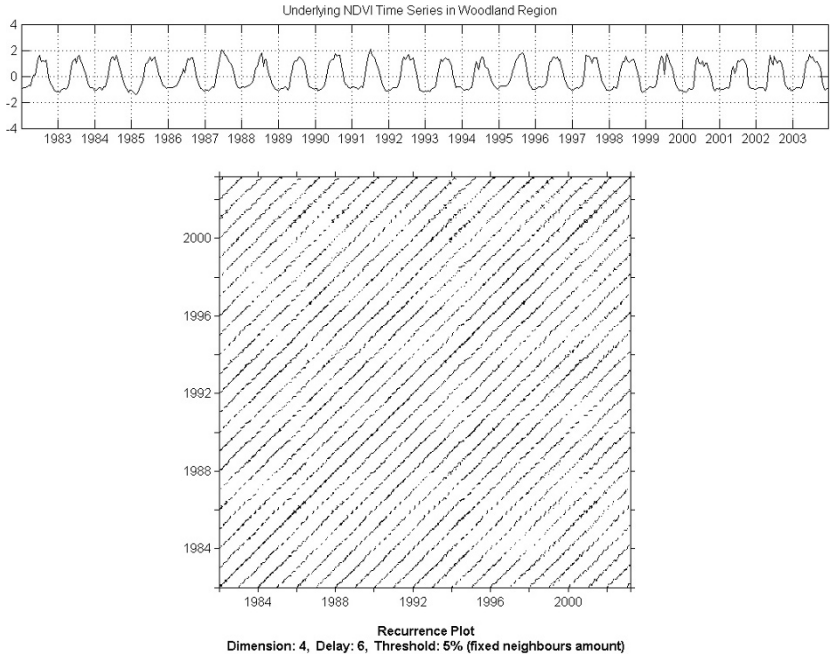

Fig. 6. The RPs of NDVI time series for woodland region.

4.2 The spatial pattern of determinism of NDVI time series

Different levels of determinism over the Beijing region show striking geographical patterning. The statistical values of *DET* in whole study area are: maximum value 79.36%, minimum value 34.83%, mean value 64.36%, and standard deviation 6.96%.

Table 3. The determinism of NDVI time series in different physical geographical regions.

Geographical Regions	MIN	MAX	RANGE	MEAN	STD
Plain in South Region	0.3484	0.7759	0.4275	0.5912	0.0648
Plateau in North Region	0.4895	0.7936	0.3042	0.6938	0.0454
Mountain in North and West Region	0.4914	0.7937	0.3023	0.6758	0.0403

By inspecting Fig. 9, it can be observed that the spatial distribution of *DET* exhibits significant regional differentiation, characterizing by lower values in the south plain region and higher values in the north mountainous and plateau regions (Table 3).

The result of overlay analysis in ArcGIS confirms that the spatial pattern of *DET* for NDVI series of study area is consistent with the spatial distribution of landuse and landcover. The lower values are found in resident area and cropland types, while higher values in woodland and grassland types (Table 4), suggesting human disturbances are responsible for the observed decline of determinism in vegetation dynamics.

Table 4. The determinism of NDVI time series in different landuse types.

Landuse types	MIN	MAX	RANGE	MEAN	STD
woodland	0.4101	0.7937	0.3836	0.6769	0.0472
grassland	0.4024	0.7881	0.3857	0.6691	0.0492
cropland	0.3863	0.7676	0.3813	0.6049	0.0678
residential area	0.3541	0.7674	0.4133	0.6242	0.0634

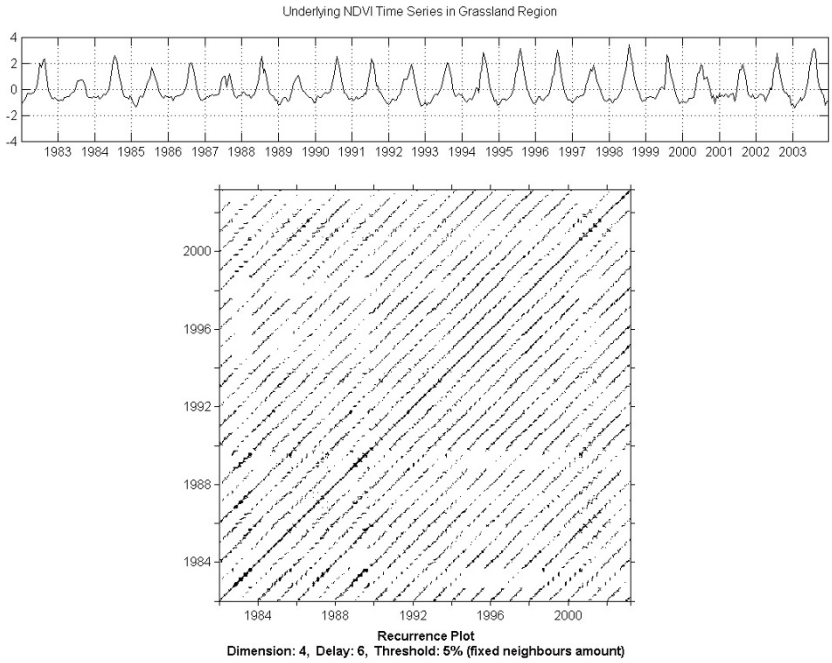

Fig. 7. The RPs of NDVI time series for grassland region.

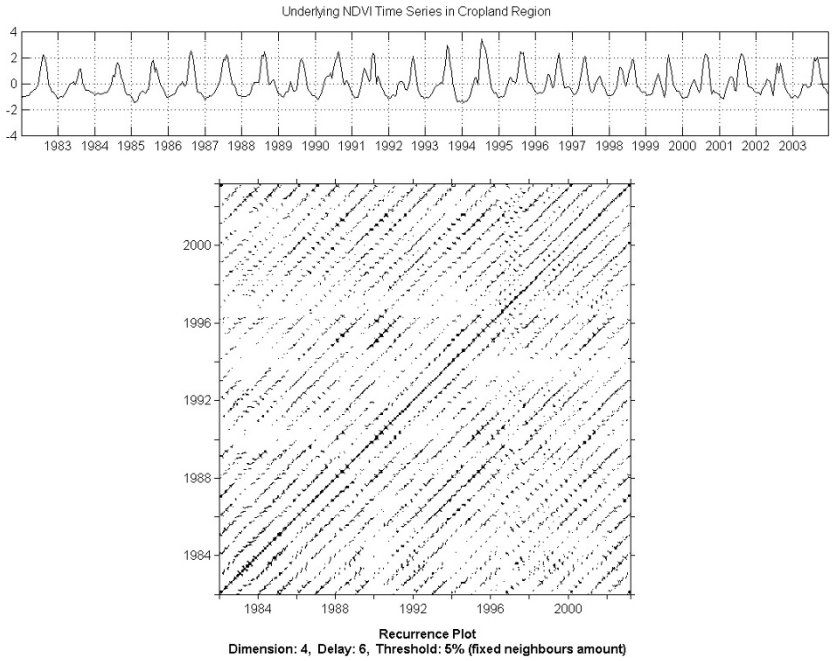

Fig. 8. The RPs of NDVI time series for cropland region.

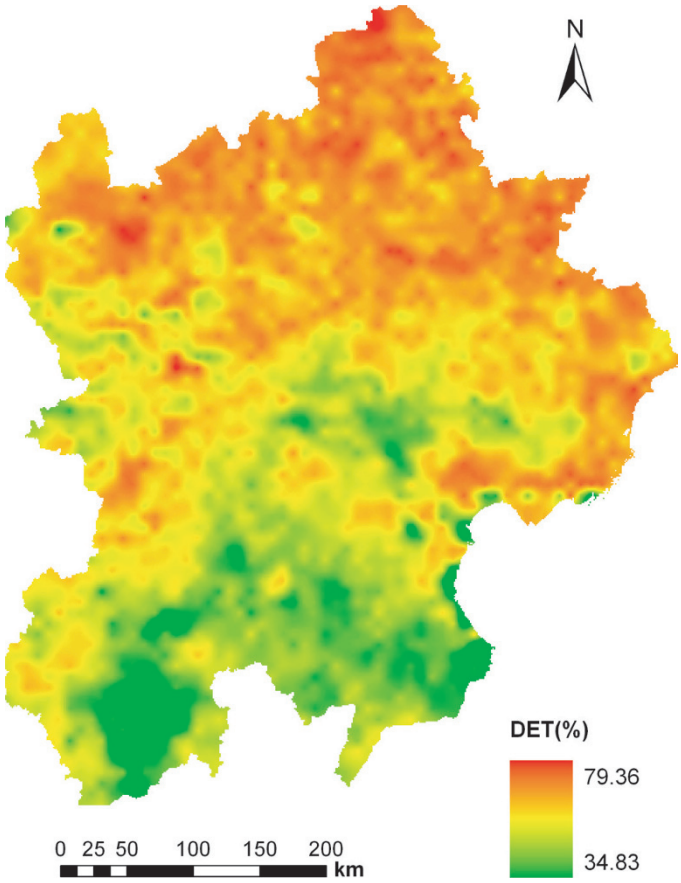

Fig. 9. The spatial pattern of *DET*.

4.3 The spatial pattern of predictability of NDVI time series

As mentioned in section 3.1, a larger K_2 value means higher unpredictability. Similar to those in Fig. 9, the spatial pattern of predictability of NDVI time series also shows significant regional differentiations and landuse/landcover associations that corroborate results obtained for determinism. As can be seen in Fig. 10, spatial patterns differ between the physical geographical regions (Table 5), as well as between the different landuse and land cover (Table 6).

Table 5. The predictability of NDVI time series in different physical geographical regions.

Geographical Regions	MIN	MAX	RANGE	MEAN	STD
Plain in South Region	0.0374	0.5070	0.4696	0.1945	0.0228
Plateau in North Region	0.0560	0.2714	0.2154	0.1770	0.0141
Mountain in North and West Region	0.0368	0.4076	0.3708	0.1813	0.0176

5 Conclusions and discussion

The objective of this paper is to demonstrate the use and applicability of recurrence plots and recurrence quantification analysis to describe trends in vegetation cover dynamics and the spatial pattern. The performance of RQA-based indices, *DET* and K_2, for representing the determinism and predictability of NDVI series, was examined respectively by using multi-temporal NOAA/AVHRR data of the region around Beijing, China. Moreover, the structures in recurrence plots for the selected NDVI series were visually inspected.

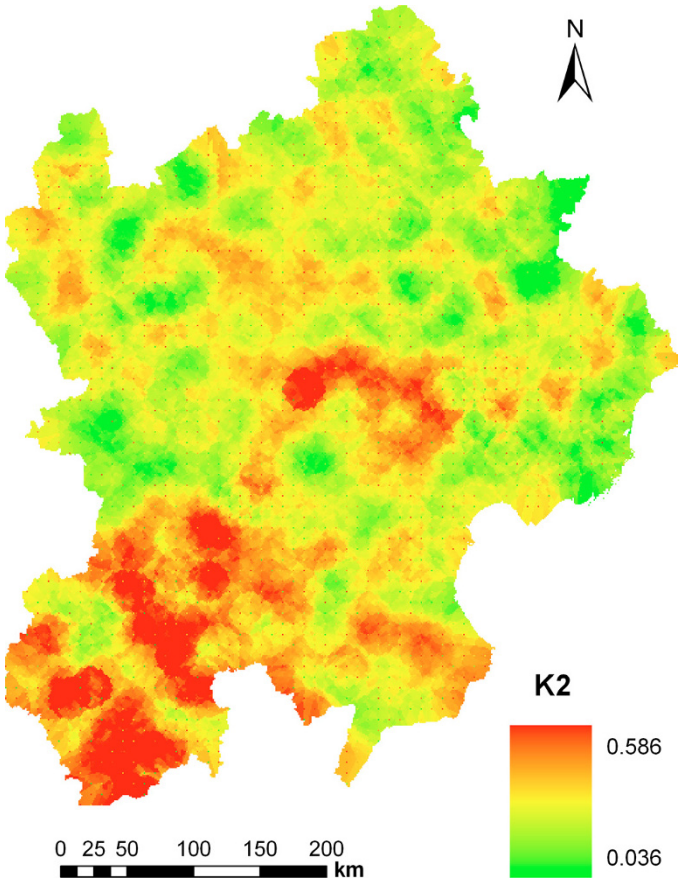

Fig. 10. The spatial pattern of K_2.

Table 6. The predictability of NDVI time series in different landuse types.

Landuse types	MIN	MAX	RANGE	MEAN	STD
woodland	0.0530	0.4076	0.3546	0.1839	0.0195
grassland	0.0467	0.2733	0.2266	0.1788	0.0167
cropland	0.0374	0.5784	0.5410	0.1942	0.0229
residential area	0.0467	0.2907	0.2440	0.1881	0.0190

The results indicate that the recurrence plots of all selected NDVI series have similar global pattern, e.g., relative non-interrupted diagonal lines and less isolated points, which suggest NDVI series are deterministic signals with stochastic noise, but more detailed difference in RPs textures was found as the differentiation of landcover and landuse types, reflecting the heterogeneity in influencing factors of NDVI series variation and its response dynamics. By carefully investigating recurrence plots of the selected NDVI series we concluded that natural ecosystems such as woodland and grassland etc. have higher determinism and predictability than artificial ecosystems e.g., city or semi-human ecosystems e.g., cropland.

By computing, interpolating and displaying RQA-based indices, DET and K_2, the spatial patterns of variation in NDVI series were examined. The spatial patterns of DET and K_2 show significant regional differentiation, i.e., lower DET or higher K_2 in the south plain region and higher DET or lower K_2 in the north mountainous and plateau regions, indicating DET and K_2 are good indicators for identifying the determinism and predictability NDVI series and their spatial patterns.

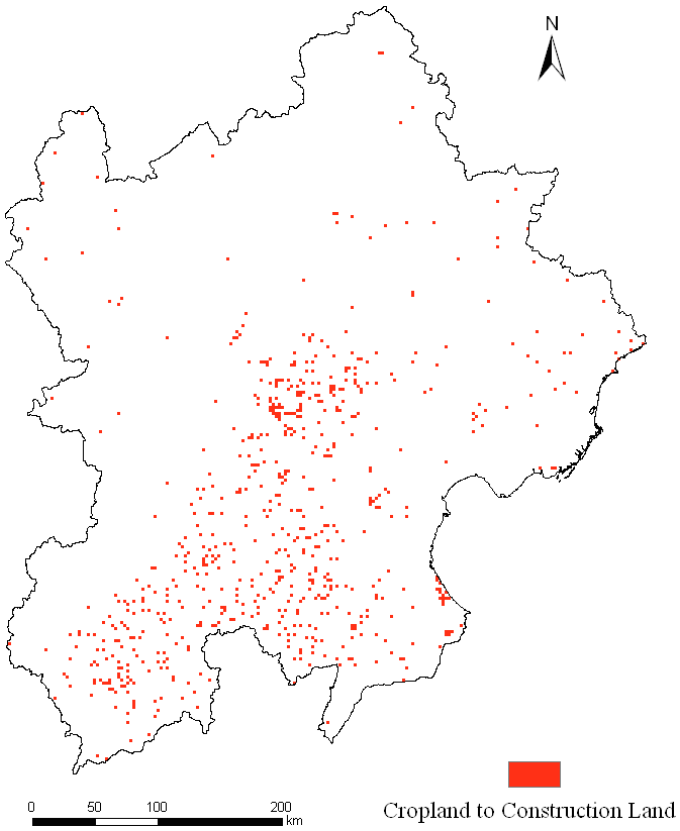

Fig. 11. Conversion from cropland to construction land from 1985 to 2000.

The spatial patterns of determinism and predictability we observed in this study may stem from the human disturbance. Compared with change of landuse and land cover of study area from 1985 to 2000 (Fig. 11), one can find that a large amount of cropland (about 15% of total cropland) especially in south plain was converted into construction land due to overpopulation and quick economic development. Moreover, plantation structure was frequently modified, resulting in the increase of randomness of NDVI series. Additionally, land cover of cropland region exhibits significant seasonality due to farming activities. The cropping period of annual crops from seeding to harvesting was typically three to four months, NDVI changed in time more rapid in comparison with the case of natural vegetation [25].

An attempt to visualize the RQA indices in geographically referenced data formats suggest that the combination of RPs and Geographical Information System is a useful approach not only in displaying the spatial patterns of RQA-based indices, but also in analyzing causal relationships between pattern and influencing factors by using powerful spatial analysis function, and thus can extend the application of RPs algorithm family to real geographical space.

Our results also have important implications for the vegetation management. In cropland and residential areas, vegetations are extensively disturbed by human activities, leading to a decrease of determinism in NDVI time series. The fact that less determinism in some vegetation types indicates that linear prediction may be insufficient to obtain correct trend of vegetation variation, suggesting that prudential measures should be adopted in vegetation management.

Recurrence quantification analysis was done using the Cross Recurrence Toolbox developed by the Nonlinear Dynamics Group at the University of Potsdam. The authors gratefully acknowledge Dr. N. Marwan for providing access to this toolbox.

Finical Supported by Key MOE Research Project No. 306019 and National Natural Science Foundation of China, No. 40771001.

References

1. L. Parrott, Ecol. Complex. **2**, 1 (2004)
2. M. Pascual, S.P. Ellner, Ecology **81**, 10 (2000)
3. R. Proulx, Ecol. Complex. **4**, 3 (2007)
4. N. Marwan, J. Kurths, Phys. Lett. A **302**, 5 (2002)
5. H. Kantz, T. Schreiber, *Nonlinear Time Series Analysis* (Cambridge University Press, 1997)
6. C.L. Webber Jr., J.P. Zbilut, *Tutorials in Contemporary Nonlinear Methods for the Behavioral Sciences* (2005), edited by M.A. Riley, G. Van Orden (2004), p. 26 `http://www.nsf.gov/sbe/bcs/pac/nmbs/nmbs.pdf`
7. N. Marwan, M.C. Romano, M. Thiel, J. Kurths, Phys. Rep. **438**, 5 (2007)
8. C.L. Webber Jr., J.P. Zbilut, J. Appl. Phys. **76**, 2 (1994)
9. N. Marwan, M.H. Trauth, M. Vuille, J. Kurths, Clim. Dynam. **21**, 3 (2003)
10. C.J. Tucker, Remote Sens. Environ. **8**, 2 (1979)
11. J.U. Hielkema, S.D. Prince, W.L. Astle, Int. J. Remote Sens. **7**, 1499 (1986)
12. A. Soriano, J.M. Paruelo, Glob. Ecol. Biogeogr. Lett. **2**, 82 (1992)
13. R.B. Myneni, C.J. Tucker, G. Asrar, C.D. Keeling, J. Geophys. Res. **103**, D6 (1998)
14. F. Maselli, M. Chiesi, Int. J. Remote Sens. **27**, 55 (2006)
15. J. Pinzon, M.E. Brown, C.J. Tucker. *Transform: Introduction and Applications*, edited by N. Huang, Hilbert-Huang (2005), p. 167
16. J.-P. Eckmann, S.O. Kamphorst, D. Ruelle, Europhys. Lett. **4**, 973 (1987)
17. W. von Bloh, M.C. Romano, M. Thiel, Nonlinear Proc. Geoph. **12**, 471 (2005)
18. J.P. Zbilut, C.L. Webber Jr., Phys. Lett. A **171**, 3 (1992)
19. L.L. Trulla, A. Giuliani, J.P. Zbilut, C.L. Webber Jr., Phys. Lett. A **223**, 225 (1996)
20. N. Marwan, N. Wessel, U. Meyerfeldt, A. Schirdewan, J. Kurths, Rev. E. **66**, 2 (2002)
21. M. Thiel, M.C. Romano, P. Read, J. Kurths, Chaos **14**, 234 (2004)
22. M.C. Romano, M. Thiel, J. Kurths, W. von Bloh, Phys. Lett. A **330**, 214 (2004)
23. A.M. Fraser, H.L. Swinney, Phys. Rev. A **33**, 2 (1986)
24. H.D.I. Abarbanel, R. Brown, J.J. Sidorowich, L.S. Tsimiring, Rev. Mod. Phys. **65**, 4 (1993)
25. S. Uchida, 22nd Asian Conference on Remote Sensing (Singapore, 2001)